ARTICLE

Rheological implications of embedded active matter in colloidal gels

Received 00th January 20xx, Accepted 00th January 20xx

DOI: 10.1039/x0xx00000x

Megan E. Szakasits,*a Keara T. Saud,^b Xiaoming Mao,^c and Michael J. Solomon^a

Colloidal gels represent an important class of soft matter, in which networks formed due to strong, short-range interactions display solid-like mechanical properties, such as a finite low-frequency elastic modulus. Here we examine the effect of embedded active colloids on the linear viscoelastic moduli of fractal cluster colloidal gels. We find that the autonomous, out-of-equilibrium dynamics of active colloids incorporated into the colloidal network decreases gel elasticity, in contrast to observed stiffening effects of myosin motors in actin networks. Fractal cluster gels are formed by the well-known mechanism of aggregating polystyrene colloids through addition of divalent electrolyte. Active Janus particles with a platinum hemisphere are created from the same polystyrene colloids and homogeneously embedded in the gels at dilute concentration at the time of aggregation. Upon addition of hydrogen peroxide – a fuel that drives the diffusiophoretic motion of the embedded Janus particles – the microdynamics and mechanical rheology change in proportion to the concentration of hydrogen peroxide and the number of active colloids. We propose a theoretical explanation of this effect in which the decrease in modulus is mediated by active motion-induced softening of the interparticle attraction. Furthermore, we characterize the failure of the fluctuation-dissipation theorem in the active gels by identifying a discrepancy between the frequency-dependent macroscopic viscoelastic moduli and the values predicted by microrheology from measurement of the gel microdynamics. These findings support efforts to engineer gels for autonomous function by tuning the microscopic dynamics of embedded active particles. Such reconfigurable gels, with multi-state mechanical properties, could find application in materials such as paints and coatings, pharmaceuticals, selfhealing materials, and soft robotics.

Introduction

Active matter is common in nature; examples include the flocking of birds, the swarming of bacteria, or the contraction of actin filaments in the cytoskeleton1-3. There has been recent interest in developing synthetic active particle systems on the nano and colloidal scale for applications such as drug delivery, sensors, or soft robotics^{4,5}. At a single particle level, active motion leads to self-propulsion of the particle⁶. There are several mechanisms for generating active motion, such as light, electric fields, or chemical potential gradients^{4,5,7}. A frequently used active particle system is the selfdiffusiophoretic transport of platinum coated Janus colloids that are activated by hydrogen peroxide⁶. Platinum catalyzes the decomposition of hydrogen peroxide (H₂O₂) into H₂O and O2; the decomposition generates a concentration gradient around the particle because of its Janus feature. This local concentration gradient leads to self-propulsion.

^a Department of Chemical Engineering, University of Michigan, Ann Arbor.

When used in self-assembly, active motion can create dynamic and reconfigurable structures that are inaccessible to purely Brownian suspensions. Active motion has been used to make living crystals comprised of dynamic aggregates that can be manipulated through light and magnetic fields^{1,2}. Combining particle anisotropy with active motion leads to more complex assemblies such as the rotating crystalline phases formed from rotating gear-like particles⁸. Furthermore, mixtures of active and passive particles have produced phenomena such as phase separation⁹, coherent clustering¹⁰, and the formation of transient lanes¹¹. Active motion can also be used to alter the equilibrium structures formed by passive particles. For example, it can enhance crystallinity by increasing the mobility of particles at grain boundaries, which promotes annealing¹².

Less work has focused on the effects of active motion on the rheology of colloidal suspensions. The mechanical response of active bacterial suspensions has been studied 3,13,14 . Adding a small fraction of active bacteria ($\phi \simeq 10^{-3}$) to water caused no change in the solution viscosity despite super-diffusive behavior of the bacteria, as characterized through one and two-point microrheology 14 . However, measurements of higher concentrations of bacteria showed a decrease in viscosity due to activity 13 .

b. Department of Materials Science and Engineering, University of Michigan, Ann Arbor.

^{c.} Department of Physics, University of Michigan, Ann Arbor.
Electronic Supplementary Information (ESI) available: [details of any supplementary information available should be included here]. See DOI: 10.1039/x0xx00000x

In addition, actin gels activated by myosin motors and adenosine triphosphate (ATP) have been studied ^{15,16}. In these systems, the addition of activity leads to an increase in the modulus of the gel network. The explanation for the observed behavior is that myosin motors apply an internal, isotropic stress (i.e. tension) to the actin network. This internal tension causes the actin network to become more rigid ¹⁵.

Activity is a promising method to alter the rheology of colloidal assemblies or to create materials with dynamic or reconfigurable mechanical properties¹⁷. Here, we investigate the effects of active motion on the rheology of colloidal gels. Colloidal gels are a state of soft matter characterized by attractively bonded particles immobilized in a network^{18,19}. Gels have useful rheological properties, such as low-frequency linear elasticity and a yield stress^{20,21}. Controlling these properties is important to industrial applications of gels including their use in food, paints and coatings, as well as in pharmaceutical products and agricultural formulations^{20,22,23}. The specific type of colloidal gel we study here are fractal cluster gels, produced by slow aggregation of dilute concentrations of polystyrene latex. These gels are good approximations of commercial materials; well-tested theory that relates gel microstructure, dynamics, and macroscopic rheology is available for fractal cluster gels^{19,24,25}.

Active particles embedded within colloidal gels could allow for the creation of gels with multi-state mechanical properties through addition and depletion of the active component. Previous research has shown that active particles embedded within colloidal gels increase the microscopic dynamics of the gel network^{26,27}. At least for a fully passive (Brownian) system, such an increase in dynamics would induce a decrease in the elastic modulus of the gel²⁴. This connection arises because the mean squared displacement of particles in the gel is related to its modulus through a generalized Stokes-Einstein equation. However, the use of this equation to relate dynamics to mechanical properties assumes that the system obeys the fluctuation-dissipation theorem, in which the energy imparted to a particle through Brownian fluctuations is dissipated through viscous drag forces²⁸. Because active motion is out of equilibrium, there is no expectation that colloidal gels with active colloids obey the fluctuation dissipation theorem; in fact, failure of the fluctuation dissipation theorem have been previously reported in active actin gels¹⁵.

In this work, we introduce active motion into colloidal gels and explore how activity affects the rheology of the gel network. We characterize the microdynamics and rheology of passive gels (comprised solely of Brownian particles) and active gels (comprised principally of Brownian particles with a small fraction of embedded active Janus colloids). We find the addition of active motion leads to a decrease in both the elastic and viscous modulus of the gel. We characterize the change in the modulus as a function of the active energy input, which is controlled by the ratio of active to passive particles and the concentration of hydrogen peroxide. We generate theoretical understanding of the modulus decrease by exploring active-motion induced softening of the spring

constant of a pair bonds of the network; this spring constant controls the gel elastic modulus. We confirm the failure of the fluctuation-dissipation theorem by comparing the measured microdynamics to mechanical rheology through the generalized Stokes-Einstein equation.

Materials and methods

Preparation of colloidal gels

Gels were self-assembled by addition of 64 mM MgCl₂, a divalent salt that induces slow aggregation, to an initially stable suspension of Janus and polystyrene colloids (1.0 ± 0.031 µm carboxylate modified polystyrene microspheres, purchased from Thermo Fisher Scientific). Janus particles were synthesized by spin coating the polystyrene colloids onto cleaned glass slides and depositing a 10 nm platinum layer on one side of the particle through physical vapor deposition²⁹. Particles were removed from the slide and washed with DI water three times. Gels were suspended in a density-matched solvent of D₂O and H₂O through bath sonication. Janus colloids were activated by addition of hydrogen peroxide (H₂O₂), which was added at the time of self-assembly. We then added MgCl₂ solution to initiate gelation of the polystyrene and Janus colloids and vortex mixed the solution to uniformly mix the H₂O₂ and MgCl₂. An anti-foam chemical (Xiameter 1410, Dow Chemical) was used to suppress formation of oxygen bubbles from decomposition of H₂O₂ ^{30,31}.

Special care was taken to ensure a uniform distribution of Janus colloids within the gel network by balancing sedimentation of the Janus colloids and gelation time. To minimize the effects of sedimentation, we deposited a thin layer of platinum onto the Janus colloids to lower their density. We also control the gelation time of the polystyrene colloids through the concentration of MgCl₂ solution. We confimed uniformity of the Janus colloid distribution in the gel by measuring their relative frequency as a function of the axial height.

The activity of the Janus colloids was characterized by direct measurement of their active dynamics as free particles (cf. SI Fig 1a). The active energies, characterized from the magnitude of the free active colloid velocity following the formulation of the swim pressure described by Takatori et al.³², are listed in SI Fig1b.

Confocal microscopy imaging of gel structure and dynamics

Gel structure and dynamics were imaged with a confocal laser-scanning microscope (Nikon A1Rsi, NA = 1.4, 100x objective). The imaging device was an 8 well chamber slide (purchased from Thermo Fisher Scientific). Two channels were used to image the fluorescent polystyrene (561 nm) and reflective platinum coatings (488 nm). Dynamic measurements were collected at a frame rate of 15 fps at 5 locations within the sample spaced 100 μm apart in the shape of a cross. Time series were processed using Trackpy, a Python implementation of the Crocker and Grier algorithm³³³,³⁴. The pixel size was 83 nm for time series images and 124 nm for 3D volumes; the

image size was 512 x 512 pixels and the number of slices in the 3D volumes was $^{\sim}$ 200. Gel structure was characterized in three dimensions using a python implementation of a watershed image analysis algorithm³⁵. The uniform spatial distribution of Janus colloids in the gels was confirmed by calculating the distribution of Janus particles as a function of height above the coverslip. The static error in the dynamics measurements is 15 nm, as determined by the method of Savin and Doyle³⁶.

Rheological characterization of gels

Rheological measurements were performed with an Anton Paar MCR 702 rheometer. Passive gel rheology was characterized using a 50 mm stainless steel parallel plate with Peltier temperature-controlled plate and hood. Samples were quickly loaded onto the rheometer after the addition of MgCl₂ solution to allow quiescent gelation of the polystyrene colloids. This sample loading time (2-3 minutes) is much shorter than the gelation time of the polystyrene colloids (15-20 minutes). To measure active gel rheology, special care is taken to suppress foaming of the suspension due to bubbles generated by the platinum-catalyzed decomposition of H₂O₂, We address this requirement by attaching polydimethylsiloxane (PDMS) films of thickness ~ 1.5 mm to the steel plates of the rheometer tooling, SI Fig 2. These PDMS films have high oxygen permeability; they were found to prevent nucleation and growth of oxygen bubbles during active gel measurements³⁷, by acting as a sink for oxygen products.

PDMS films are made by mixing a 10:1 ratio of polymer to crosslinker (Dow Sylgard 182 or 184) and cured at 100°C for 4 hours in a Teflon mold ³⁷. The PDMS is attached with epoxy (Devcon 2 ton epoxy) to sandpaper with adhesive backing. To ensure the uniform spreading of the PDMS, a 4 kg weight is applied during the setting period of the epoxy. The epoxy is cured for at least one hour and the PDMS-sandpaper film is attached to the steel rheometer fixtures. We compare the accuracy of the PDMS coated plates to traditional stainless steel plates by measuring a frequency sweep with a solution of 4.0 wt. % polyethylene oxide (PEO, Polysciences Inc. MW = 106) in water, SI Figure 4, and find no significant discrepancy between the fixtures coated with PDMS film and the standard stainless steel fixtures.

The temperature of all rheological measurements is 20°C . The strain amplitude for measurements is 0.003, confirmed to be in the linear regime (cf. Figure 2c and Figure 6) for both passive and active gels. We characterize the rheology of the passive gel with a 50 mm stainless steel fixture at a gap of 500 μ m. We performed a gap study and found there are no significant gap effects above 500 μ m, SI Figure 5. We chose to use a gap of 500 μ m to conserve sample material. A sandblasted (rough) steel fixture was used to confirm the absence of slip in the experiments of this study, SI Figure 6.

We estimate the lower stress limits of the rheometer through two methods: 1) experimentally through oscillatory strain sweeps and 2) calculated from the lower torque limit of the rheometer. We performed oscillatory strain sweeps with PEO solutions at 1.0, 2.0, and 4.0 wt. % to determine the lower stress/strain limits of the rheometer, SI Figure 7. At the strain amplitude used for all rheology measurements (γ = 0.003), the lowest resolvable elastic modulus is G' = 0.01 Pa. We also calculate the lowest resolvable modulus from the minimum torque of the rheometer, $G = \frac{2T}{\pi R^3 \gamma}$ = 0.02 Pa, where T is the lower torque limit, R is the radius of the plate, and γ is the strain amplitude³⁸. Both methods give similar estimates of the lowest resolvable modulus. All data reported in this manuscript are at or above limits calculated from both methods.

Frequency-dependent microrheological characterization

The mean-squared displacement (MSD) of all particles in the gel was computed from particle trajectories, as determined by Trackpy³³³. We use the generalized Stokes-Einstein equation to compute the linear viscoelastic storage and loss moduli, $G'(\omega)$ and $G''(\omega)$ respectively. They are extracted from a Fourier transform of the MSD following methods described in Dasgupta et al³³. Microrheological measurements were compared to small amplitude oscillatory shear measurements performed with mechanical rheology. These measurements were performed after the gel had equilibrated quiescently in the rheometer for 15 minutes.

Results

Fractal cluster structure of active gels

The gels are self-assembled with a dilute fraction of platinum-coated Janus colloids dispersed uniformly in them; the Janus particles are activated by the presence of hydrogen peroxide (H_2O_2). Figure 1 compares a projection of the 3D structure of these active gels to gels without incorporated Janus particles — what we refer to as passive gels. The gels are imaged with a 10x, 40x, and 100x microscope objective at a t = 60 minutes after the initiation of gelation. At large magnification levels (100x), the fractal structure of the gel is present in both the passive and active gels. As the magnification is decreased, the gel structure in both cases appears progressively more uniform and fluid-like, consistent with the transition from fractal to cluster structure in these gels at increasing scales⁴⁰.

To quantify the gel structure, we calculate the fractal dimension, d_f , and average cluster size, R_c , from measurements of the radial distribution function, $g(r)^{41,42}.$ Specifically, the fractal dimension of the passive gels is $d_f=1.8\pm0.1$, and their cluster size is $R_c=19\pm5~\mu m$. The fractal dimension of the active gels is $d_f=1.9\pm0.1$ and average cluster size is $R_c=21\pm7~\mu m$. We compare p values obtained from 2 sample T-tests and find the differences in d_f (p = 0.29) and R_c (p = 0.71) between active and passive gels are not statistically significant. In both active and passive gels, d_f is approximately 1.8, consistent with previously reported values for gels formed through diffusion limited cluster aggregation $^{24,25}.$

We observe that the introduction of the active Janus particles during gelation does not significantly affect the large-scale microstructure of the gel. In our experiments, phase separation is not observed, as seen in previous studies of mixtures of active and passive colloids⁹. This difference is likely due to the attractive forces that drive gelation dominating; these strong and short-range interactions drive the formation of a frozen microstructure with active particles uniformly distributed throughout the cluster structure. Recent work from Omar et. al., studied the effects of embedding active colloids within a gel while varying the swim force. In their simulations, they found that at lower active energies, the embedded active particles are unable to alter the gel structure²⁷.

Macroscopic rheology of passive fractal gels

Figure 2 shows the values of the elastic (G') and viscous (G") moduli as a function of time, frequency, and strain for a fractal cluster gel comprised of purely passive particles. Transient measurements were performed at a fixed frequency $\omega=1.0$ rad/s and strain $\gamma=0.003$. We find that G' and G" reach quasi-steady states value of G' = 0.15 \pm .08 Pa and G" = 0.13 \pm 0.06 Pa at t $^{\sim}$ 20 minutes. Colloidal gels of this kind undergo aging; however, the time scale for our experiments (t = 15-60 min) is shorter than the timescales for aging (t $^{\sim}$ several days) 43 . The strain sweep in Figure 2c shows that the linear regime of the gel structure persists until a strain amplitude of $\gamma \sim$ 0.01. The transition from linear to non-linear rheological behavior is consistent with previous studies of colloidal gels, where the onset of nonlinearity is a consequence of bond breaking 21,44 .

The addition of H_2O_2 to the passive gels stiffens the network by a factor of about 40% (c.f. SI Fig 8), resulting in $G'=0.5\pm0.2$ Pa and $G''=0.3\pm0.2$ Pa. Such gel stiffening in the presence of H_2O_2 , a strong oxidizer, has been previously reported and described as the modest consequence of its physical chemical effect on the pair potential interaction between the colloids²⁶. To account for the effects of H_2O_2 stiffening the passive gel network, we compare active gels to passive gels with H_2O_2 included, consistent with the approach of ref [26].

Macroscopic rheology of active fractal gels

Active gel rheology was characterized using the PDMS-modified rheometer fixtures. Figure 3 shows a) G' and b) G'' as a function of time for H_2O_2 concentrations varying from 5% to 10% and for a ratio of active to passive particles at $\frac{N_{active}}{N_{total}} = 0.12$. We find that the introduction of activity causes a decrease in both G' and G'' when compared to gels comprised of purely passive particles. The linear viscoelastic moduli furthermore decrease with increasing concentration of hydrogen peroxide. The amount of decrease is significant, with a factor of 8.5 drop in modulus relative to the passive gel observed at the highest H_2O_2 concentration studied. Measurements in Figure 3c were acquired 30 minutes after the initiation of gelation; the full range of H_2O_2 concentrations

studied is plotted in SI Figure 10. The modulus measured at the highest concentration of hydrogen peroxide ($G' \sim 0.04$ Pa) is still greater than the lowest resolvable modulus determined from instrument sensitivity measurements (SI Figure 11). There is some variability in the monotonically decreasing trend apparent at low H_2O_2 concentrations.

To observe the effect of Janus particle fraction on the modulus change, the concentration of hydrogen peroxide is fixed at 2.5% and the active to passive particles ratio varied from 0.05 to 0.14, as reported in Figure 4. Increasing the abundance of active particles in the gel also leads to a progressively greater decrease in the elastic modulus of the gel network; there is one data set that does not follow the decreasing trend ($\frac{N_{active}}{N_{total}}$ = 0.12). Although anomalous, this data set is included in the subsequent analysis and modelling.

We note that because a chemical fuel (H_2O_2) drives the active motion and modulus decrease, the observed effect of activity is expected to decline as that fuel is consumed. However, given estimates of H_2O_2 decomposition kinetics on platinum, the number of Janus particles, and the surface area of platinum on the particles, the depletion of the fuel should occur at times $^{\sim} 10^5$ s, 6,45,46 well outside the timescale of the measurements reported here.

Macroscopic rheology as a function of the active energy

To generalize our results to any active particle system and not specifically to one in which the activity is generated by platinum-catalyzed decomposition of hydrogen peroxide - we plot the modulus as a function of the energy of the active colloids, E_A . The energy of an active colloid is taken as: $E_A =$ ξ VI, where ξ is the hydrodynamic drag, V is its velocity, and l is the run length of an active particle, given by $l= au_R V$. The active particle run length is a function of V and the Brownian reorientation time, $au_R = rac{8\pi\eta a^3}{k_BT}$, where η is the viscosity of the solvent and a is the particle radius 26,32 . This energy characterizes the energy dissipated during the ballistic motion of the particle over the time scale where the particle orientation randomly changes. Over the range of H₂O₂ concentrations used in this study, we find that each active particle engages in dynamics equivalent to an energy that is 3 - 9 times greater than the thermal energy (cf. SI Figure 1b). This approach has been previously applied to characterize the microdynamics of active gel networks²⁶.

To account for the joint effects of the ratio of active colloids and the H_2O_2 concentration, we plot G' and G'' as a function of $(X_AE_A+X_PE_P)/E_P$, where X_A,X_P are the number fraction of particles which are active or passive $(X_A+X_P=1)$, and $E_P=k_BT$ is the thermal energy which characterizes fluctuations of the passive particles. The combination $(X_AE_A+X_PE_P)/E_P$ represents a weighted average of energy scales of fluctuations of the colloidal particles, normalized by the thermal energy. This weight-averaged energy acts as an "effective temperature" to the gel and controls the pair potential, as we discuss below.

Figure 6 shows the ratio of the active to passive gel viscoelastic moduli, $\frac{G_A}{G_P}$, as a function of $(X_AE_A+X_PE_P)/E_P$. The rheology data from both varying the ratio of active to passive particles and varying the concentration of H_2O_2

collapse on to a single curve, and the modulus of the gel network decreases with increasing energy provided by the active colloids. This collapse indicates that the weight-averaged energy correlates the rheology of the active gels; this collapse will be applied in the next section to model the results.

Towards a mechanism for activity induced modulus decrease

The following potential explanations of the measurements were evaluated and found to be inconsistent with the observed decrease in the moduli: first, since the fractal cluster gelation process occurs with active particles present, the activity of the Janus particles could generate a different fractal cluster structure, with a weaker, lower modulus gel formed in the presence of Janus particles relative to the passive gel in which Janus particles were absent. This possibility is inconsistent with the observation that the active and passive gel fractal cluster structures are similar, as apparent in Figure 1, and the differences in $d_{\rm f}$ and $R_{\rm c}$ for the passive and active gels are also not statistically significant.

A second possible explanation is accelerated gel aging/syneresis induced by the embedded active colloids; this aging could, for example, be generated by the enhanced vibrational dynamics of the active colloids ²⁶. Previous work has shown that syneresis leads to the formation of a more compact gel structure with slower dynamics^{43,47}. However, such behavior would most likely lead to an increase in the modulus (as is, for example, observed previously for passive gels⁴⁸), which is the opposite of what is observed in the active gel rheological measurements.

Finally, an active-motion induced change in the linear region of the gels' response to small amplitude oscillatory shear could explain the measurements. All linear measurements in this study are at fixed strain amplitude, $\gamma=0.003$; if active motion reduced the linear region below this value, a lower apparent modulus might be found for the active gels. Figure 5 shows there is only a modest shift in the onset of non-linearity for an active gel (5% $\rm H_2O_2$) when compared to the passive gel ($\gamma_{NL,passive} \sim 0.07$ vs. $\gamma_{NL,active} \sim 0.03$); however the strain used for our measurements ($\gamma=0.003$) remains well below the strain amplitude for nonlinearity of the active gel.

Active motion induced changes in the spring constant

Having found that active motion does not significantly affect measures of the gel network structure, we examine how dynamical changes in the gel network induced by active motion could affect the viscoelastic moduli. The increase in gel dynamics due to activity can lead to stretched bonds between pairs of particles; in this case the interaction potential would be softened. As we discuss below, this leads to a decrease in the spring constant of bonds in the gel network, which controls the elastic moduli²⁴.

The pairwise interaction potential between the colloidal particles is not a simple harmonic potential with the spring constant being a "constant". Instead, as a sum of the Van der Waals attraction and the screened electrostatic repulsion, it is a potential that softens as the inter-particle distance r

increases. This effect can be shown by calculating the effective spring constant of the potential, which is a function of the energy level of the fluctuation between this pair.

For a pair of passive particles, this effective spring constant is extracted from the potential through:

$$k_{passive} = \frac{k_B T}{\langle r^2 \rangle_{th} - \langle r \rangle_{th}^2} \tag{1}$$

where

$$\langle A \rangle_{th} = \int_0^\infty dr \, A \, e^{-V(r)/k_B T} / \int_0^\infty dr \, e^{-V(r)/k_B T}$$

$$(2)$$

represents the canonical ensemble average over thermal fluctuations, and V(r) is a sum of the screened electrostatic repulsion and the van der Waals attraction between the colloids, see Supplemental Information. The rationale behind this spring constant calculation is that with thermal fluctuations, the particle-pair explores a finite range of rinstead of just staying at the minimum, and the effective spring constant should describe the fluctuation of the interdistance in a way that $k_{passive}\langle(\delta r)^2\rangle_{th}\sim k_BT$, is satisfied. This can also be more rigorously shown by calculating the linear response of a pair under fluctuations to external force, as discussed in Rocklin et. al.⁴⁹. For this particular potential, this calculation yields $k_{passive} = 0.008 \, N/m$. This value is smaller than the curvature at the minimum of the potential, which gives $k_0 =$ $0.016 \, N/m$, but at the same order of magnitude. A way to understand this is that the potential well is the steepest near the minimum and becomes weaker as r increases.

When active energy is injected into the system, fluctuation of the pair distance r increases. Inspired by the scaling collapse using the parameter of $(X_AE_A+X_PE_P)/E_P$, we describe this effect through the mean-field picture of an effective temperature

$$T_{eff} = (X_A E_A + X_p E_p)/k_B \tag{3}$$

where k_B is the Boltzmann constant. The idea behind this effective temperature is that the active Janus particles are bonded to passive particles, so their active motion causes an active strain field, which drags the passive particles to also fluctuate more²⁶. This effect can be captured in a mean-field way through this effective temperature.

This definition of the effective temperature is particular to colloidal particles bonded in a gel network, where the particle-position fluctuations are much smaller than the run length of a free particle. In this case, $E_A = \xi V l$ represents the active energy that drives the particle from its equilibrium positions. Other ways to define the effective temperature, such as through the diffusivity⁵⁰, has been used in the literature to describe free active particles. The resulting effective

temperature is of the same order of magnitude but with a different geometric factor. In all cases the active energy leads to a smaller effective spring constant

$$k_{eff} = \frac{k_B T_{eff}}{\langle r^2 \rangle_{eff} - \langle r \rangle_{eff}^2} \tag{4}$$

where $\langle \cdot \rangle_{eff}$ represents the canonical ensemble average at temperature T_{eff}

$$\langle A \rangle_{eff} = \int_0^\infty dr \, A \, e^{-V(r)/k_B T_{eff}} /$$

$$\int_0^\infty dr \ e^{-V(r)/k_B T_{eff}} \tag{5}$$

This spring constant is smaller than $k_{passive}$ due to the anharmonicity of the interaction potential, as illustrated in Fig. 6. This is an approximate way to estimate the effective spring constant using equilibrium statistical ensembles.

The macroscopic shear moduli G' and G" are then proportional to this effective spring constant k_{eff} which is a function of the ratio $\frac{X_AE_A+X_PE_P}{E_P}=\frac{T_{eff}}{T}$. Fig. 6 shows the normalized effective spring constant $k_{eff}/k_{passive}$ as a function of T_{eff}/T , calculated using Eqs. (1-2), and the result agrees very well with the rheological measurement in the same plot. Experimental data shown in Fig 6 were collected 30 minutes after initiation of gelation. For completeness, comparison between the experimental data at 15, 30 and 60 minutes after initiation of gelation and the effective spring constant are shown in Figure S12. The calculations of the effective spring constant correlate best with the experimental data at 15 and 30 minutes, with higher deviations apparent at longer times.

Connecting microscopic dynamics to macroscopic rheology

We compare the measured decrease in active gel elastic modulus with the increased microscopic displacement of colloids in the gel network, by means of a generalized Stokes-Einstein equation

$$G^*(\omega) = \frac{k_B T}{\pi a i \omega \Im\{\langle x^2(\tau) \rangle\}}$$
 (6)

where $G^*(\omega)$ is the complex shear modulus, a is the particle radius, and $< x^2(\tau) >$ is the ensemble averaged mean squared displacement (MSD) 39 . This approach has been used to characterize the viscoelastic properties of colloidal gels⁵¹. Specifically, the model developed by Krall and Weitz is based on measurements of the gel's microdynamics as determined by dynamic light scattering²⁴.

We compute the MSD of the gel network, $< x^2(\tau) >$, at 0, 15, 30, and 60 minutes after addition of salt to induce particle gelation, as shown in Figure S13. The MSD of the gel network increases with an increase in the H_2O_2 concentration, consistent with previous reports²⁶. The frequency-dependent elastic modulus determined from the MSD through the generalized Stokes-Einstein equation (hereafter referred to as microrheology), are reported in Figure 7.

We focus on values of $G'(\omega)$ and $G''(\omega)$ obtained from microrheology and macroscopic rheological measurements at 15 minutes after the addition of salt, and in the low frequency limit (the full data set is reported in SI). The frequency-dependent viscoelastic moduli, as characterized through mechanical rheology, show that the decrease in the viscoelastic moduli due to activity holds over a wide frequency range. We calculate the power law scaling exponent (α) from the macroscopic frequency sweeps, $G \sim \omega^{\alpha}$. We find α is independent of the H_2O_2 concentration. The invariance of α between passive and active gels further suggests that the active motion does not affect the microstructure of the gel⁵².

To compare the microdynamics with mechanical rheology, we chose the low-frequency range of the measurements to accommodate the fact that most theory connecting microdynamics and mechanical rheology has been developed in this limit ⁴⁹. Comparison of Figure S15 shows that the generalized Stokes-Einstein equation appears to hold for the passive gels at low-frequency. (The situation is less clear at higher frequency, as shown in the SI.)

Figure 7 shows G' and G" as a function of H₂O₂ concentration at a fixed frequency (0.5 s-1), obtained from micro and macro rheology. The mechanical rheology measurements show a greater decrease in the modulus with increasing H₂O₂ concentration. That is, the microdynamics yield an overestimate of the linear viscoelastic moduli relative to that obtained from mechanical rheology. This situation holds at all H₂O₂ concentrations. Therefore, in the lowfrequency range addressed here, the generalized-Stokes Einstein equation fails to connect the low-frequency microdynamics of the active gel to the elastic moduli from mechanical rheology, contrary to the measurements for the passive gels. That is, although activity causes microscopic fluctuations of the colloids to increase, the softening of the elastic modulus due to activity occurs to a greater extent than the fluctuation magnitude would lead one to expect, as predicted by the fluctuation dissipation theorem.

Conclusions

Embedded active colloids decrease the linear viscoelastic moduli of fractal cluster colloidal gels. The amount of decrease is a function of the total active energy input, which is itself dependent on the ratio of active to passive colloids and the energy of the active Janus particles. The active energy of the Janus particles is set by the concentration of H_2O_2 . The magnitude of the moduli decrease due to the embedded active colloids is significant: At an active particle concentration of $\sim 14\%$, the moduli decrease by a factor of 8.5.

We compared the low-frequency moduli of the gels, as measured by microrheology and mechanical rheometry and as connected by the generalized Stokes-Einstein equation. The two sets of measurements agree well for passive gels at low frequencies, consistent with the generalized Stokes-Einstein equation; however, there is a discrepancy as large as a factor of four between the microrheology and mechanical rheology. That is, the mechanical rheometry records a lower elastic

modulus than microrheology predicts from the microdynamics measurements and application of the generalized Stokes-Einstein equation. This comparison confirms that the generalized Stokes-Einstein equation does not hold in fractal cluster gels with embedded active matter, a clear indication that the fluctuation – dissipation theorem fails in this system ⁵³. The nature of this breakdown is a fruitful avenue for future research; this work provides data that specifies the out-of-equilibrium relationship between the microscopic fluctuations in the active gel system to the measured rheology.

In previous work, active actin gels were shown to violate the fluctuation dissipation theorem due to contractile forces the myosin motors apply to the actin network¹⁵. In these gels, myosin motors act as active crosslinks; they make the gels more rigid^{15,16}. Studies of active gels concluded that the activity of the myosin motors leads to contraction and stiffening of the active actin gels – an outcome equivalent to modulus enhancement. On the other hand, in this study, we find that fractal cluster gels with embedded active particles display a softened, rather than stiffened, rheological response. The opposite behavior in the two systems (modulus decrease vs increase) is likely due to both the nature of the active motion in the two as well as differences in how the active matter interacts with the passive network structure. Specifically, myosin motors are able to translate along the actin filaments, altering the structure of the actin gels, and they have a "stall force" to lock the network in the stressed state. In the active gels studied in this article, the active particle is bound to the gel network through attractive forces that are stronger than the active energy. The active particles furthermore can undergo random reorientation as the network structure fluctuates, thereby affecting the direction of the active force. Thus, the effect of activity in the gels works to enhance, rather than suppress, random fluctuations. This enhancement serves to soften the gel, rather than the alternative, in which fluctuations are suppressed through the generation of a static tension, which serves to stiffen the gel.

We explored several potential mechanisms to describe the origin of the decrease in the moduli in the active fractal cluster gels. We conceptualize possible effects of active motion into two primary categories: one in which the active motion changes the gel network structure itself and the other in which active motion acts to change dynamical features of the gel network. As discussed in the results, changes in the structure of the gel network, including variations in the fractal structure and accelerated syneresis, were not observed in our experiments. In the current study, we compared the fractal structure through measurements of the fractal dimension and average cluster size. Future work could probe for subtle effects of the effects of active motion on the microstructure of colloidal gels through other measures such as connectivity. Future modeling efforts designed to incorporate collective or rigidity effects would benefit from such additional microstructural characterization^{54–57}. We do observe an (at most) modest shift in the onset of non-linear rheological behavior in the active gels. However, all measurements were performed at low enough strain amplitudes ($\gamma = 0.003$) to

afford high confidence that linear rheological behavior was probed.

The scaling collapse and the quantitative agreement between theory and experiment of Figure 6 support the second scenario, wherein the active motion increases the fluctuations of the active colloids. These fluctuations couple to surrounding colloids and soften the inter-particle potential in the gel network, and thereby function to lower the elastic moduli. Future work can address: (1) the specific coupling mechanism between the dynamics of the active and passive particles in the gel. This work has applied a mean-field approach; however, other approaches are possible [24] and measurements of correlated microdynamics could resolve the specifics of the mechanism. (2) The relationship between microscopic fluctuations and macroscopic response in active The work has demonstrated that the fluctuationgels. dissipation theorem fails for active fractal cluster gels. The macroscopic rheological response is impacted by the active colloids to a much greater degree than the microscopic dynamics and the generalized Stokes-Einstein equation would predict. Particle-level simulation of active gels could identify the governing physics in this case.

Conflicts of interest

There are no conflicts to declare.

Acknowledgements

We acknowledge T. F. Scott for discussions regarding the PDMS plate and J. A. Ferrar for discussions about the anti-foam chemicals. We acknowledge Anton Paar for providing instruments through a loan program. M. E. S. acknowledges support by a Rackham Merit Fellowship. This work is supported by NSF CBET-1702418 and NSF CMMT-1609051. This work was performed in part at the University of Michigan Lurie Nanofabrication Facility.

References

- B. M. Mognetti, a. Šarić, S. Angioletti-Uberti, a. Cacciuto, C. Valeriani and D. Frenkel, *Phys. Rev. Lett.*, 2013, **111**, 1–5.
- J. Palacci, S. Sacanna, A. P. Steinberg, D. J. Pine and P. M.
 Chaikin, *Science* (80-.)., 2013, 339, 936–940.
- 3 E. J. Hemingway, A. Maitra, S. Banerjee, M. C. Marchetti, S. Ramaswamy, S. M. Fielding and M. E. Cates, *Phys. Rev. Lett.*, 2015, **114**, 1–5.
- S. J. Ebbens and J. R. Howse, Soft Matter, 2010, 6, 726– 738.
- 5 S. Sánchez, L. Soler and J. Katuri, *Angew. Chemie Int. Ed.*, 2015, **54**, 1414–1444.
- J. R. Howse, R. A. L. Jones, A. J. Ryan, T. Gough, R.
 Vafabakhsh and R. Golestanian, *Phys. Rev. Lett.*, 2007, 99, 048102.
- W. F. Paxton, S. Sundararajan, T. E. Mallouk and A. Sen, *Angew. Chemie Int. Ed.*, 2006, **45**, 5420–5429.

- 8 N. H. P. Nguyen, D. Klotsa, M. Engel and S. C. Glotzer, *Phys. Rev. Lett.*, 2014, **112**, 075701.
- J. Stenhammar, R. Wittkowski, D. Marenduzzo and M. E.
 Cates, *Phys. Rev. Lett.*, 2015, 114, 1–5.
- 10 D. P. Singh, U. Choudhury, P. Fischer and A. G. Mark, *Adv. Mater.*, 2017, **29**, 1–7.
- S. McCandlish, A. Baskaran and M. Hagan, *Soft Matter*, 2012, 8, 2527–2534.
- B. van der Meer, L. Filion and M. Dijkstra, 2016, 12, 3406–3411.
- 13 H. M. López, J. Gachelin, C. Douarche, H. Auradou and E. Clément, *Phys. Rev. Lett.*, 2015, **115**, 1–5.
- 14 D. T. N. Chen, A. W. C. Lau, L. A. Hough, M. F. Islam, M. Goulian, T. C. Lubensky and A. G. Yodh, *Phys. Rev. Lett.*, 2007, **99**, 1–4.
- 15 D. Mizuno, C. Tardin, C. F. Schmidt and F. C. MacKintosh, *Science (80-.).*, 2007, **315**, 370–373.
- T. B. Liverpool, M. C. Marchetti, J.-F. Joanny and J. Prost, *Europhys. Lett.*, 2009, **85**, 18007.
- 17 M. J. Solomon, *Langmuir*, 2018, **34**, 11205–11219.
- V. Prasad, V. Trappe, A. D. Dinsmore, P. N. Segre, L. Cipelletti and D. A. Weitz, *Faraday Discuss.*, 2003, **123**, 1–12.
- 19 E. Zaccarelli, J. Phys. Condens. Matter, 2007, 19, 323101.
- L. C. Hsiao, R. S. Newman, S. C. Glotzer and M. J. Solomon,
 Proc. Natl. Acad. Sci., 2012, 109, 16029–16034.
- 21 W.-H. Shih, W. Y. Shih, S.-l. Kim, J. Liu and I. A. Aksay, *Phys. Rev. A*, 1990, **42**, 4772–4779.
- R. Mezzenga, P. Schurtenberger, A. Burbidge and M. Michel, Nat. Mater., 2005, 4, 729–740.
- 23 M. H. Lee and E. M. Furst, *Phys. Rev. E*, 2008, **77**, 041408.
- 24 A. H. Krall and D. A. Weitz, *Phys. Rev. Lett.*, 1998, **80**, 778–781
- 25 M. Lattuada, H. Wu and M. Morbidelli, *Chem. Eng. Sci.*,2004, **59**, 4401–4413.
- 26 M. E. Szakasits, W. Zhang and M. J. Solomon, *Phys. Rev. Lett.*, DOI:10.1103/PhysRevLett.119.058001.
- 27 A. K. Omar, Y. Wu, Z. G. Wang and J. F. Brady, ACS Nano, 2019, 13, 560–572.
- W. B. Russel, D. A. Saville and W. R. Schowalter, *Colloidal Dispersions*, Cambridge University Press, 1989.
- 29 A. A. Shah, B. Schultz, K. L. Kohlstedt, S. C. Glotzer and M. J. Solomon, *Langmuir*, 2013, **29**, 4688–4696.
- 30 Z. Németh, G. Rácz and K. Koczo, *J. Colloid Interface Sci.*, 1998, **207**, 386–394.
- 31 A. J. O'Lenick, J. Surfactants Deterg., 2000, **3**, 229–236.
- 32 S. C. Takatori, W. Yan and J. F. Brady, *Phys. Rev. Lett.*, 2014, **113**, 028103.
- D. Allan, L. Uieda, F. Boulogne, R. W. Perry, T. A. Caswell and N. Keim, , DOI:10.5281/zenodo.12255.
- J. Crocker and D. Grier, J. Colloid Interface Sci., 1996, 310,
 298–310.
- 35 L. C. Hsiao, B. A. Schultz, J. Glaser, M. Engel, M. E. Szakasits,

- S. C. Glotzer and M. J. Solomon, *Nat. Commun.*, 2015, **6**, 8507.
- 36 T. Savin and P. S. Doyle, *Biophys. J.*, 2005, **88**, 623–638.
- D. Dendukuri, D. C. Pregibon, J. Collins, T. A. Hatton and P.S. Doyle, *Nat. Mater.*, 2006, 5, 365–369.
- 38 Ewoldt, Randy H., M. T. Johnston and L. M. Caretta, in Complex Fluids in Biological Systems, 2015, pp. 207–241.
- B. R. Dasgupta, S.-Y. Tee, J. C. Crocker, B. J. Frisken and D.
 A. Weitz, *Phys. Rev. E*, 2002, **65**, 051505.
- M. Carpineti and M. Giglio, *Phys. Rev. Lett.*, 1992, **68**,
 3327–3330.
- 41 M. Lattuada, H. Wu, A. Hasmy and M. Morbidelli, *Langmuir*, 2003, **19**, 6312–6316.
- 42 M. Lattuada, H. Wu and M. Morbidelli, J. Colloid Interface Sci., 2003, 268, 106–120.
- 43 L. Cipelletti, S. Manley, R. C. Ball and D. A. Weitz, *Phys. Rev. Lett.*, 2000, **84**, 2275–2278.
- 44 H. J. Walls, S. B. Caines, A. M. Sanchez and S. A. Khan, *J. Rheol. (N. Y. N. Y).*, 2003, **47**, 847–868.
- 45 D. W. McKee, J. Catal., 1969, 14, 355–364.
- M. A. Hasnat, M. M. Rahman, S. M. Borhanuddin, A. Siddiqua, N. M. Bahadur and M. R. Karim, *Catal. Commun.*, 2010, 12, 286–291.
- 47 S. Mazoyer, L. Cipelletti and L. Ramos, *Phys. Rev. Lett.*, 2006, **97**, 8–11.
- 48 G. Yin and M. J. Solomon, *J. Rheol. (N. Y. N. Y).*, 2008, **52**, 785–800.
- 49 D. Z. Rocklin, L. C. Hsiao, M. Szakasits, M. J. Solomon and X. Mao, arXiv Soft Condens. Matter, 2018, 1–7.
- J. Palacci, C. Cottin-Bizonne, C. Ybert and L. Bocquet, *Phys. Rev. Lett.*, 2010, **105**, 088304.
- 51 a M. Puertas and T. Voigtmann, *J. Phys. Condens. Matter*, 2014, **26**, 243101.
- 52 H. H. Winter and F. Chambon, *J. Rheol. (N. Y. N. Y).*, 1986, **30**, 367–382.
- 53 T. A. Waigh, Reports Prog. Phys., 2005, **68**, 685–742.
- 54 M. Zupkauskas, Y. Lan, D. Joshi, Z. Ruff and E. Eiser, *Chem. Sci.*, 2017, **8**, 5559–5566.
- J. M. Drake, P. Levitz, S. K. Sinha and J. Klafter, *Chem. Phys.*, 1988, **128**, 199–207.
- A. D. Dinsmore and D. A. Weitz, *J. Phys. Condens. Matter*,2002, 14, 7581–7597.
- 57 S. Zhang, L. Zhang, M. Bouzid, D. Z. Rocklin, E. Del Gado and X. Mao, *Phys. Rev. Lett.*, 2019, **123**, 058001.

ARTICLE

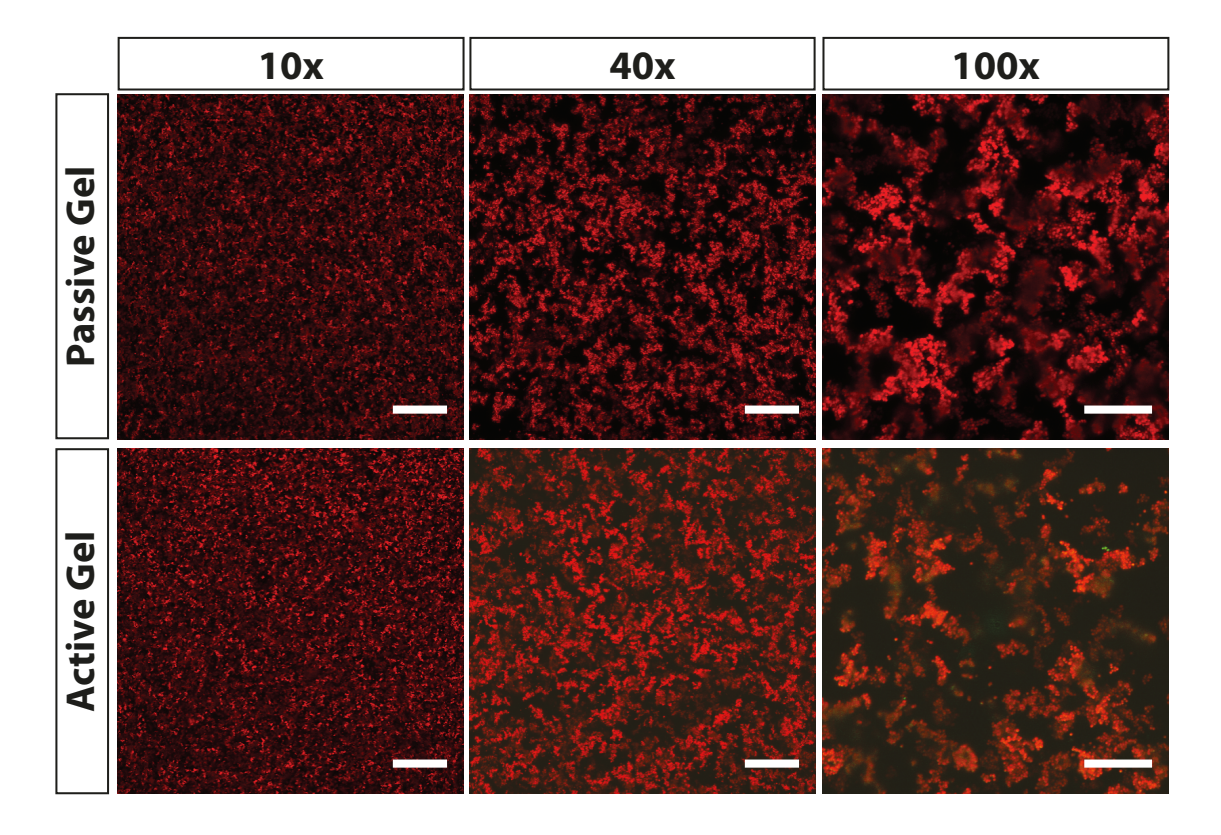


Figure 1. Passive and active gel structure across multiple length scales, imaged 60 minutes after initiation of gelation. Scale bar for 10x objective is 200 μ m, 40x objective is 50 μ m, and 100x objective is 25 μ m.

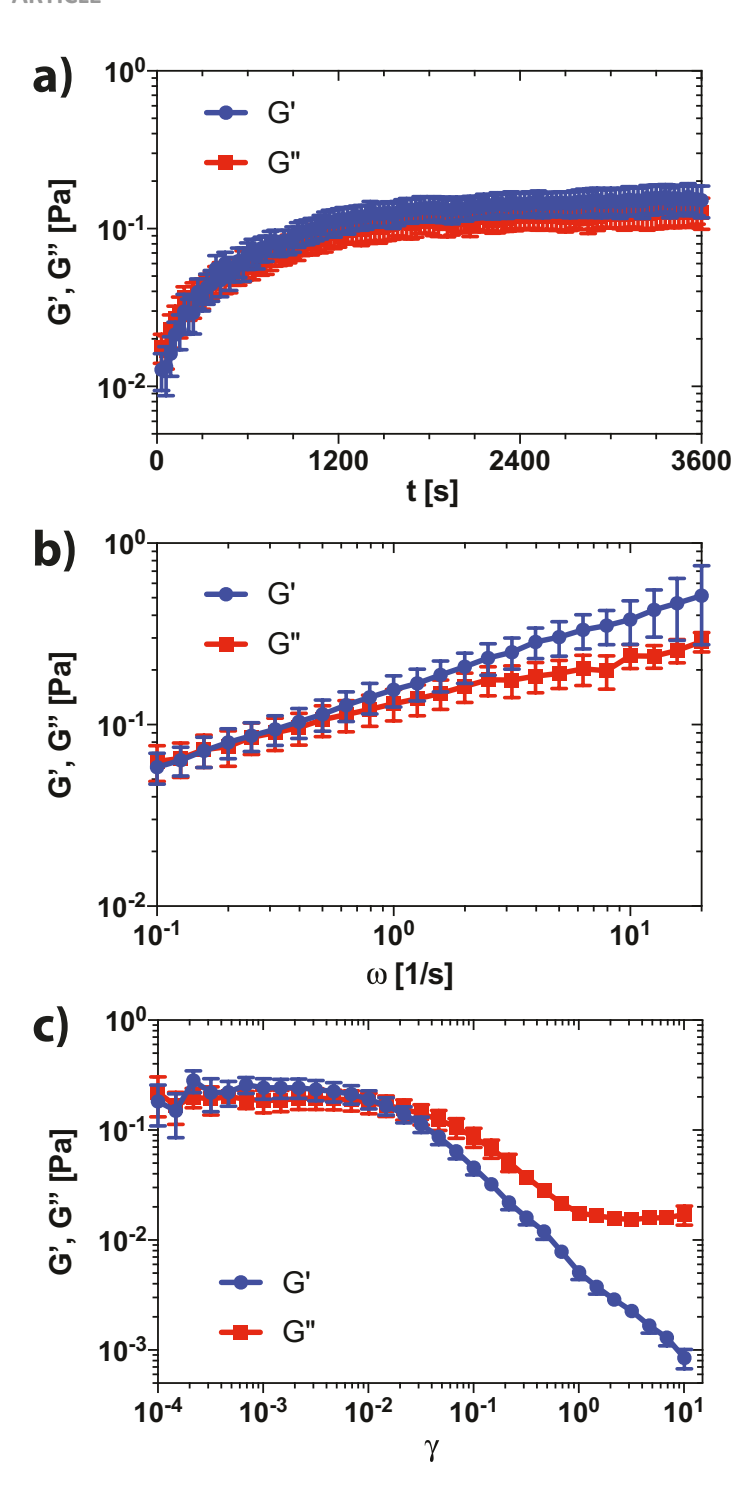


Figure 2. Passive gel storage and loss moduli (G', G'') as a function of a) time at γ = 0.003 and ω = 1 s⁻¹; b) frequency at γ = 0.003 and t = 1 hour, and c) strain at ω = 1.0 s⁻¹ t = 1.5 hours.

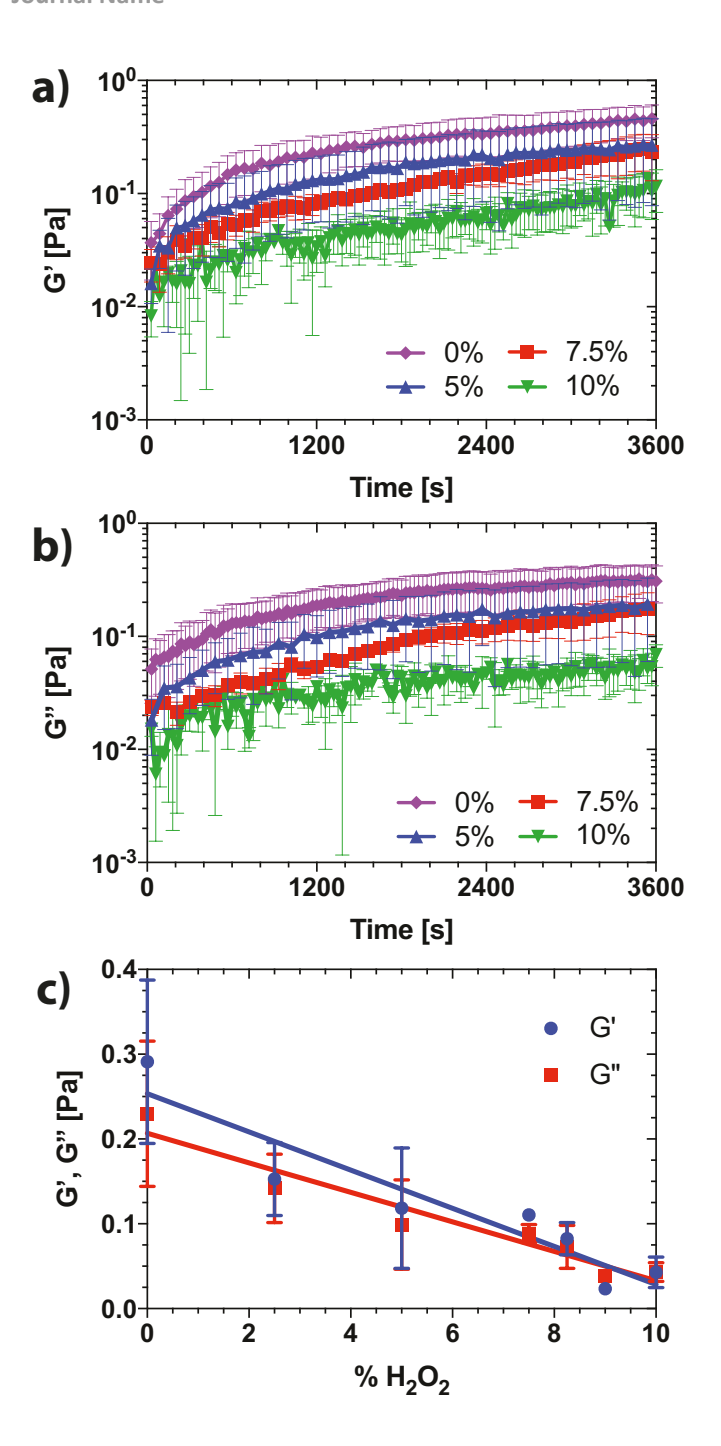


Figure 3. Active gel rheology at a fixed ratio of active to passive particles ($X_A = .12$) as a function of the concentration of H_2O_2 . a) Elastic and b) viscous moduli as a function of time at each H_2O_2 concentration. c) G', G'' as a function of the H_2O_2 concentration at t = 1800 s. Measurements were performed at a fixed strain amplitude ($\gamma = 0.003$) and frequency ($\omega = 1.0 \text{ s}^{-1}$).

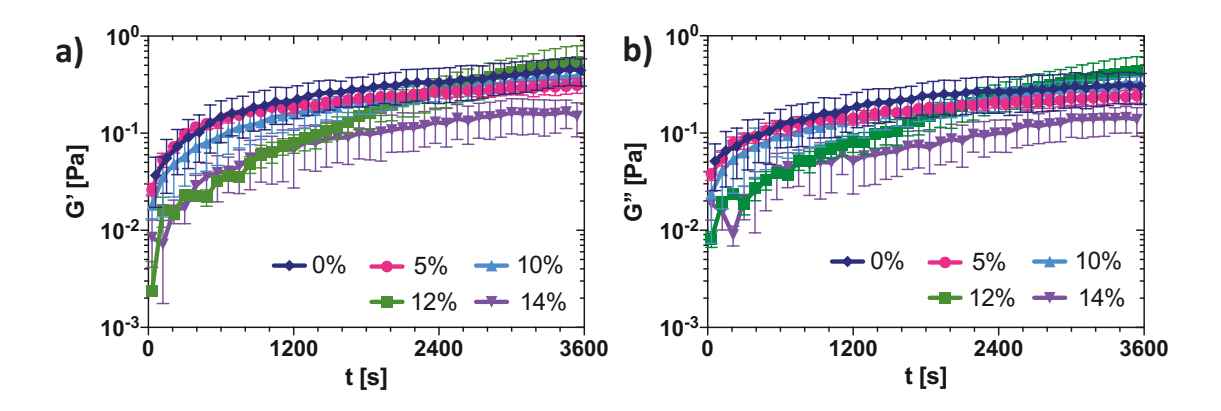


Figure 4. Transient linear rheological response of active gels at fixed concentration of hydrogen peroxide (2.5%) and a function of the ratio of active to passive particles. a) Elastic and b) viscous moduli are plotted as a function of time at a fixed strain (γ = 0.003) and frequency (ω = 1.0 s⁻¹).

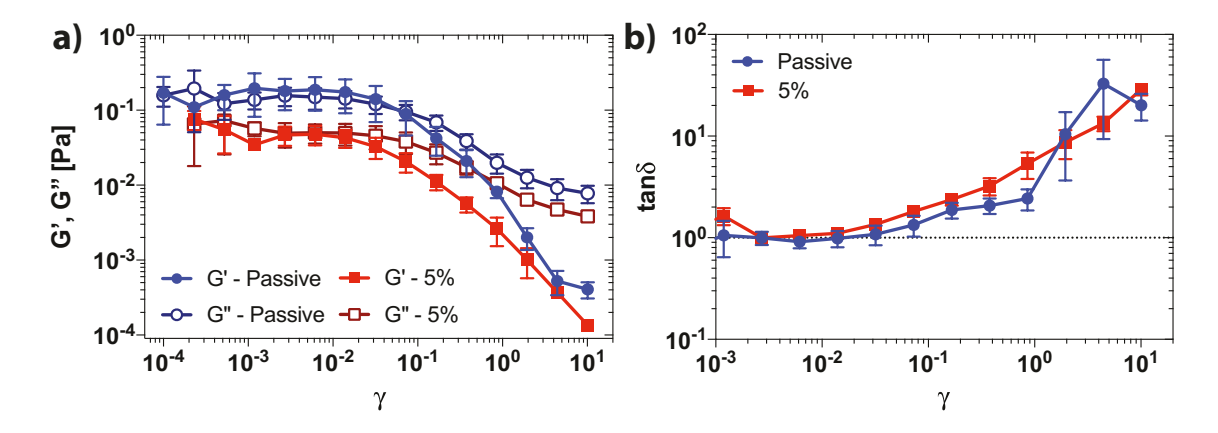


Figure 5. Strain amplitude sweep of passive and active gels, with 5% H_2O_2 and active to passive colloid ratio, $X_A = 0.12$; a) G' and G'' and G''

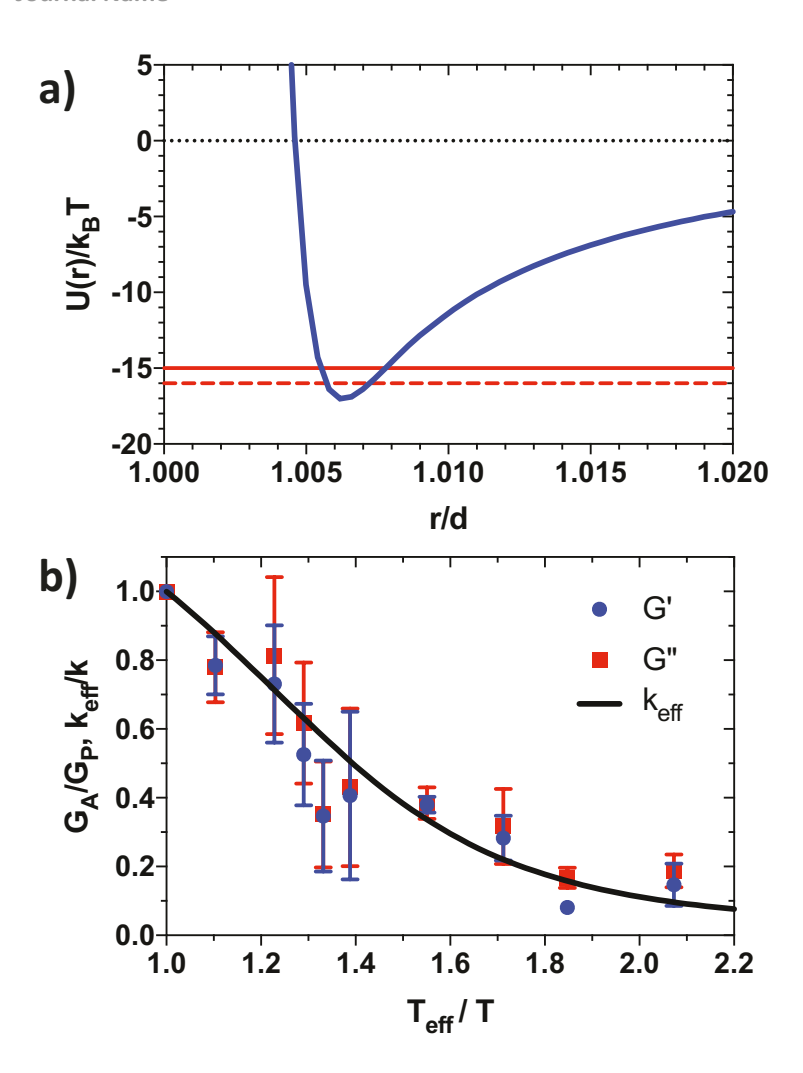


Figure 6. a) Pair potential for colloidal particles - based on van der Waals and charge interactions - as a function of the center-to-center separation, r, normalized by the particle diameter (blue curve). The red dashed line shows the level of thermal fluctuations, k_BT , from the potential minimum, and the red solid line shows the level of fluctuations of the active energy at $\frac{T_{eff}}{T} = 2$. Anharmonicity of the pair potential leads to the softening of the effective spring constant as fluctuation increases. b) Ratio of passive to active gel viscoelastic moduli and spring constant as a function of the active energy.